PHYSICAL REVIEW B VOLUME 29, NUMBER 3 1 FEBRUARY 1984

Studies of the intermittent-type chaos in ac- and dc-driven Josephson junctions

I. Goldhirsch
Department of Fluid Mechanics and Heat Transfer, Faculty of Engineering, Tel Aviv University, Tel Aviv 69978, Israel

Y. Imry and G. Wasserman
Department of Physics and Astronomy, Tel Aviv University, Tel Aviv 69978, Israel

E. Ben-Jacob
Institute for Theoretical Physics, University of California, Santa Barbara, California 93106
(Received 24 June 1983)

The intermittent-type chaos occurring in rf- and dc-current-driven Josephson junctions is investigated numerically and analytically. A simple physical model is proposed and is used for an analytic calculation of the temporal correlation function and the power spectrum. The latter has a broadband part whose behavior near threshold is discussed. Comparison with numerical results shows good quantitative agreement. Further generalizations of this approach needed for a quantitative agreement with the numerical results are outlined. The "effective noise temperature" for the chaotic state is discussed.

I. INTRODUCTION

The small Josephson junction[1-5] driven by both ac- and dc-current sources is a relatively simple physical system which displays a wealth of nontrivial (and useful) nonlinear phenomena.[6-24] Among these is the appearance of chaos without external noise which is of fundamental interest and complicates the operation of devices. The RSJ (resistively shunted junction, or driven pendulum) model[25,26] is known to provide a qualitatively correct description of the behavior of the real junction in many cases. The same mathematical model seems to be relevant to other physical systems, such as charge-density waves[27] and various electronic circuits. The latter are sometimes used for analog simulation of the properties of the Josephson junction.[28]

A great deal of insight into the phenomena of chaotic behavior and the various routes to chaos[29-33] has been achieved through the use of simple mathematical models and recursion relations or model maps. One of the hopes or stipulations is that very simple models possess many universal properties in common with "real" chaotic systems which have a macroscopic number of degrees of freedom. The agreement between some results obtained in the investigation of the "simple" dynamical systems and some experiments on continuous systems[34] is impressive indeed. What is missing, however, is a link between simple dynamical systems and real physical systems, such as a systematic reduction procedure connecting the latter to the former. Such a procedure would enable one to identify universality classes and make further predictions related to physical systems. As a first, albeit small, step in this direction—an understanding of simple dynamic physical models with a small number of degrees of freedom seems instructive.

One of the interesting modes of chaos is that of intermittency.[29,35] A system in such a mode would typically stay for some time in an "ordered" (laminar or periodic) state, then a burst of some other (possibly, but not necessarily disordered) behavior would appear, followed by a return to the ordered state and so on. The lengths of the intervals of time between chaotic bursts are random and do not possess long-time correlations. This phenomenon has been identified in the Lorenz model[36] by Pomeau and Manneville[35] and by Yorke and Yorke.[29] Hirsch, Huberman, and Scalapino[37] have studied this phenomenon in one-dimensional maps, putting special emphasis on its threshold behavior and the effects of noise. Interesting modeling of this effect in the Lorenz model[36] appeared in a work by Aizawa.[38] The same effect was detected in the[39-41] RSJ model of the driven Josephson junction in Refs. 21, 22, and 39 and was analyzed with the aid of a model in Ref. 42. Many more systems exhibit this phenomenon—such as chemically reacting mixtures[43] or hydrodynamic systems.[34]

In the present paper we restrict ourselves mainly to the study of the intermittent properties of the RSJ model and the routes to this mode. This type of chaos is associated with frequency-locked solutions (corresponding to Shapiro steps) becoming unstable. Owing to its relevance to the physics of the Josephson junction and related devices, such as parametric amplifiers[17,18] and voltage standards,[19,20] this model has been studied quite extensively. The case of the zero-dc component was treated in Ref. 39 (with emphasis on bifurcation sequences) and in Refs. 40 and 41. Both ac- and dc-driven systems were treated in Refs. 42 and 44. Chaotic behavior and routes to chaos[39,41,44] as well as intermittency[21,22,40,42,44] were studied also. The relation of chaos with a large gain in parametric systems based on the ac Josephson effect was studied in Ref. 45.

The structure of the paper is as follows. Section II

presents a partial review of the various solutions as well as numerical results in periodic and aperiodic regimes in the steps and in chaotic regions in the gaps between the steps. Routes leading to one type of solution from others are described also. A model[38,42] for calculating the correlation functions and power spectra for the intermittent chaotic solutions is presented in Sec. III and the (small) corrections needed to improve it are discussed in Sec. IV. Remarks concerning the critical behavior close to threshold are made in Sec. V, and the effective noise temperature is discussed in Sec. VI. The results are briefly summarized in the concluding section.

II. THE MODEL AND SOME RESULTS

The RSJ model[25,26] for the small Josephson junction driven by both dc and ac current sources reads

$$\ddot{\theta}+G\dot{\theta}+\sin\theta=I+A\sin(\omega_{\rm ex}t)\ , \tag{2.1}$$

where θ is the junction's phase difference; time is measured in units of ω_J^{-1}; $\omega_J\equiv(2eI_J/\hbar C)^{1/2}$ being the Josephson plasma frequency (where I_J is the Josephson critical current of the junction); $G=(\omega_J RC)^{-1}$, R (assumed constant) is the normal resistance of the junction and C its capacitance; I and A are, respectively, the dc current and the amplitude of the ac driving current, measured in units of I_J and $\omega_{\rm ex}$ the external ac driving frequency, measured in units of ω_J; we shall denote $T\equiv 2\pi/\omega_{\rm ex}$ as the period of the forcing.

For given values of the parameters, the solutions of (2.1) usually settle, after an initial transient, into one of a typically small set of long-term "steady" (but not necessarily periodic) solutions, which may be characterized by the average value of the voltage, given via the Josephson relation by

$$\langle V\rangle=\frac{\hbar}{2e}\langle\dot{\theta}\rangle\ , \tag{2.2}$$

in ordinary units. It is convenient to use a dimensionless voltage, $v\equiv V/RI_J$ which is given in the units employed here by

$$\langle v\rangle=G\langle\dot{\theta}\rangle\ . \tag{2.2'}$$

For small G the initial conditions (e.g., θ, $\dot{\theta}$ at $t=0$) determine into which of the (possibly more than one) solutions[21,22] the system will settle.

Many of the solutions are frequency locked with respect to the external ac frequency in the sense that their average voltage satisfies

$$\langle v\rangle=\frac{n}{m}G\omega_{\rm ex}\ ,\quad n,m \text{ integers} \tag{2.3}$$

i.e., θ advances by $2\pi n$ during m periods of the external source $T_{\rm ex}$. Since these solutions may exist for a range of I, one obtains the well-known Shapiro[2] steps in the dc I-V characteristics. The $m=1$, $n>1$ steps are called harmonic, and the $m>1$ ones are subharmonic[16,21] steps. There may be infinitely many exceedingly small subharmonic steps forming a "devil's staircase" structure,[22] when no external noise[23] is added to the system. The possibility of period doubling on the steps will be discussed below. In addition to the frequency-locked solutions, there also exist solutions with unlocked frequencies in between the steps, and their $\langle v\rangle$ appears to change continuously with I. These solutions that we[21–23,42] as well as other investigators[39,40–44] have seen are not periodic. They appear to be chaotic in the sense of exhibiting a sensitive dependence at long times on small changes in the initial conditions. The ranges of chaotic solutions may be increased by enlarging the gaps between the sizeable harmonic steps. This can be done by reducing the stability of the latter. The stability of the steps was discussed in some detail in Refs. 12, 21, and 4. Generally, these chaotic solutions appear at low $\omega_{\rm ex}$ and, usually, at not-too-high values of the dissipation constant G. Estimates for real values of the parameters needed to yield chaotic solutions were given in Ref. 44. The nature of the chaotic solutions in the stability gaps of the large harmonic steps is of the intermittent type: The system stays for several cycles near the solution corresponding to the less unstable step, which is an unstable orbit in phase space, then wanders, typically for a cycle or two, into the range of the other step, following which it goes back to a cycle near the first step, etc. The "jumps" between the steps appear to be random, and they are determined by the strength of the instability of the solution corresponding to a given step. When the interstep gap is spanned by varying I, the relative stability is changed; the lower step is predominant near the lower edge of the gap, and the opposite happens near the upper edge. It may well happen that setting I close to a range of existence of an incipient not-too-small subharmonic step[21,22] within the gap may make the solution spend also some time in the vicinity of that orbit. There is some evidence for this in the (somewhat) small erratic changes in the nature of the chaotic solutions, in addition to the main changes explained above, as I is varied, but we have not examined this interesting possibility in any detail.

Another important effect that happens sometimes when the stability limit of a step is approached is a period-doubling sequence, first discovered for this model in Ref. 15 and for the pure ac case in Ref. 39 and shown numerically in certain cases to agree with the Feigenbaum sequence[30] by Kautz.[44] We have seen such effects as well (the step "1/1" becoming "2/2") in our numerical and analog simulations. Typically, the period doubling appears as a symmetry breaking of the solution where the pieces representing two consecutive original periods, T, of the solution become unequivalent so that the periodicity becomes $2T$ instead of T (see Fig. 3). However, θ advances now by 4π during a time $2T$, so that $\langle v\rangle$ stays the same. Thus the period doubling occurs *on* a given step. Since further doublings may occur employing the same mechanism (we emphasize that they, as well as the first bifurcation, do not appear to occur in all cases), they should also remain on the same step characterized by $\langle v\rangle$. Thus, the whole period-doubling sequence of the above type, if it occurs, should remain on the initial step.[40,42] In fact, even the chaotic behavior which follows immediately after the accumulation point of the period-doubling thresholds may still have a "locked" frequency and an average voltage which is still on the step. The disorder as-

sociated with this type of chaos is created by a stochastic amplitude modulation of the peaks in $\dot{\theta}$, while the associated frequency, or average v may stay locked. This kind of effect was indeed found numerically by Kautz[44] who obtained in some cases completed bifurcation sequences into a chaotic behavior *on* a particular step.[40] In addition to this, when I is increased beyond the stability limit of the whole voltage-locked step, intermittency will start since the system wanders randomly into ranges of phase space where $\dot{\theta}$ is effectively different from the "original" step. Such ranges, are, for example, the vicinity of a phase space orbit of a different step. Therefore, one finds here the very interesting possibility of two types of randomness characterizing the chaotic state—random amplitude modulation and intermittency involving frequency (or voltage) changes.

While this paper is mainly devoted to a study of the latter effect, one should be aware of the interesting possibility that the two above-mentioned mechanisms may in fact not be totally independent. The Manneville-Pomeau picture[35] associates intermittency with the proximity of a tangent bifurcation. Such a mechanism in fact occurs inside the chaotic range of the logistic map where bands of, e.g., period-three solutions exist. Such bands may be approached from the chaotic range by tangent bifurcations which are associated[37] with intermittent behavior. It is of interest to find out whether intermittency in other systems, such as ours, may be a related phenomenon. However, there is as yet no clear evidence for this correspondence in this case.[46,47] One may note, in this connection, that in the overdamped limit[6,8,11,46–49] the ensuing first-order equation may be described by a one-dimensional (1D) mapping which does display a special type of tangent bifurcation[47] and an associated aperiodic[48] solution, but with apparently no period three necessarily involved.

We now present some further results of our numerical studies of Eq. (2.1). In addition to exploratory analog simulations, the equation was solved numerically by a Runge-Kutta method with typically 30–40 integration points per cycle T. From the $\theta(t)$, $\dot{\theta}(t)$, for a given solution we constructed the phase-space orbit (where $\dot{\theta}$ vs $\cos\theta$ is a convenient representation for this problem), the Poincaré sections ($\dot{\theta}$ vs $\cos\theta$ for times successively differing by one period T), the time-correlation function of $\dot{\theta}$, $C(t)$, and its cosine Fourier transform, $S(\omega)$. $S(\omega)$ is the power spectrum of $\dot{\theta}$. $C(t)$ is defined by averaging the autocorrelation of $\dot{\theta}$

$$C(t)=\lim_{T_0\to\infty}\frac{1}{T_0}\int_0^{T_0}dt'\dot{\theta}(t')\dot{\theta}(t'+t)\ . \tag{2.4}$$

This correlation was evaluated by numerical integration over the discrete (time) points of $\dot{\theta}(t)$, where T_0 was increased up to a few hundred cycles and $C(t)$ evaluated in a range T_1 that was smaller than T_0 by about an order of magnitude. The convergence as function of T_0 was visually checked. $S(\omega)$ was defined via

$$S(\omega)=2\int_0^{\infty}C(\tau)\cos(\omega t)dt\ . \tag{2.5}$$

It was calculated numerically with a resolution $2\pi/T_1$ and an upper limit of the order of $10\omega_{ex}$. Our aim has been to understand the qualitative nature of the solution and not to get higher precision, which would necessitate much longer computations. $S(\omega)$ was also obtained by squaring the transform of $\dot{\theta}(t)$, yielding similar results.

While we have done computations for other cases as well, it is convenient to display the important features by discussing a specific range. The numerical results shown here were all obtained for

$$G=0.75,\quad \omega_{ex}=0.25,\quad A=0.4\ . \tag{2.6}$$

The relevant part of the I-V characteristics for these values of the parameters is schematically shown in Fig. 1. We shall concentrate on the range of the I inside the gap between the zeroth and the first step as well as on the portions of three steps adjacent to the gap, i.e., $0.6\lesssim I\lesssim 0.72$.

We now present some numerical results for several values of the dc current I, where for each value $C(t)$, $S(\omega)$, the phase-space plot and Poincaré section are shown. Numerical examples for the solution were displayed in Refs. 21–23 and 42.

A simple static situation, on the first step $\langle\dot{\theta}\rangle=0$, for $I=0.6$ is shown in Fig. 2. The Poincaré section is one point, the phase-space orbit is a closed curve, $C(t)$ is a periodic function, and $S(\omega)$ is a series of δ functions (within our resolution) at ω_{ex} and its integral multiples. A period-doubled $\langle\dot{\theta}\rangle=0$ solution is exhibited in Fig. 3, for $I=0.7142$. Here the Poincaré section consists of two points, the phase-space orbit has a loop, and $C(t)$ displays a "broken symmetry" with alternating larger and smaller peaks. Correspondingly, $S(\omega)$ has now also subharmonic peaks at half-integral multiples of ω_{ex}. A period-doubled case near the lower edge of step 1 ($\langle v\rangle=G\omega_{ex}$) is shown in Fig. 4 for $I=0.717$, where many of the features are qualitatively similar to the previous case except that now, since $\langle\dot{\theta}\rangle>0$, $C(t)$ has a positive average as well. This also results in a new "δ function" peak in $S(\omega)$ at the origin ($\omega=0$), which is an important feature of any $\langle v\rangle=0$ solution. The phase-space orbits in Figs. 3 and 4 do not appear to be single curves and the Poincaré points have some scatter. This appears to be beyond the numerical ac-

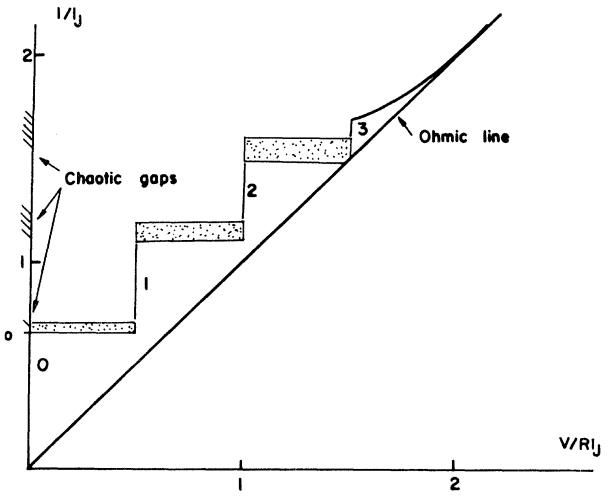

FIG. 1. A schematic I-V characteristic for Eq. (2.6).

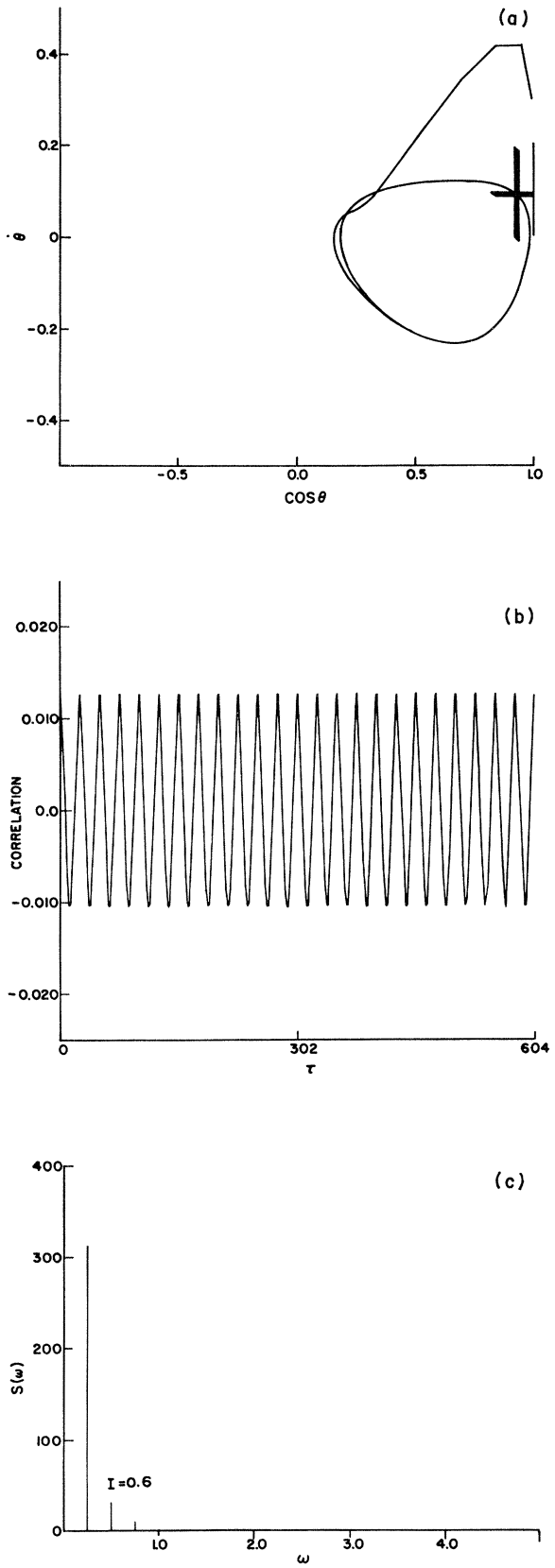

FIG. 2. (a) Phase-space plot and Poincaré section (crosses), (b) the correlation function $C(\tau)$, and (c) the power spectrum. The parameters are as in Eq. (2.6); the dc current value is $I=0.6$, a simple static solution.

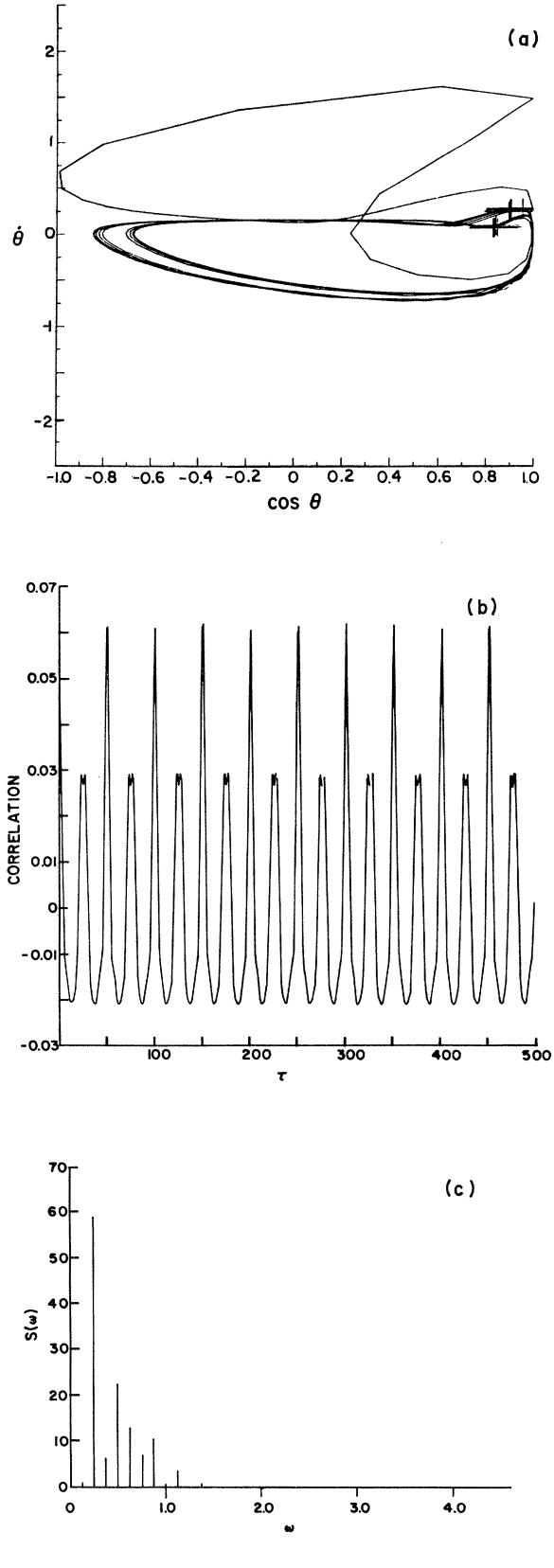

FIG. 3. (a) Phase-space plot and Poincaré section (crosses), (b) the correlation function $C(\tau)$, and (c) the power spectrum. The parameters are as in Eq. (2.6); the dc current value is $I=0.7142$, a frequency-doubled static solution.

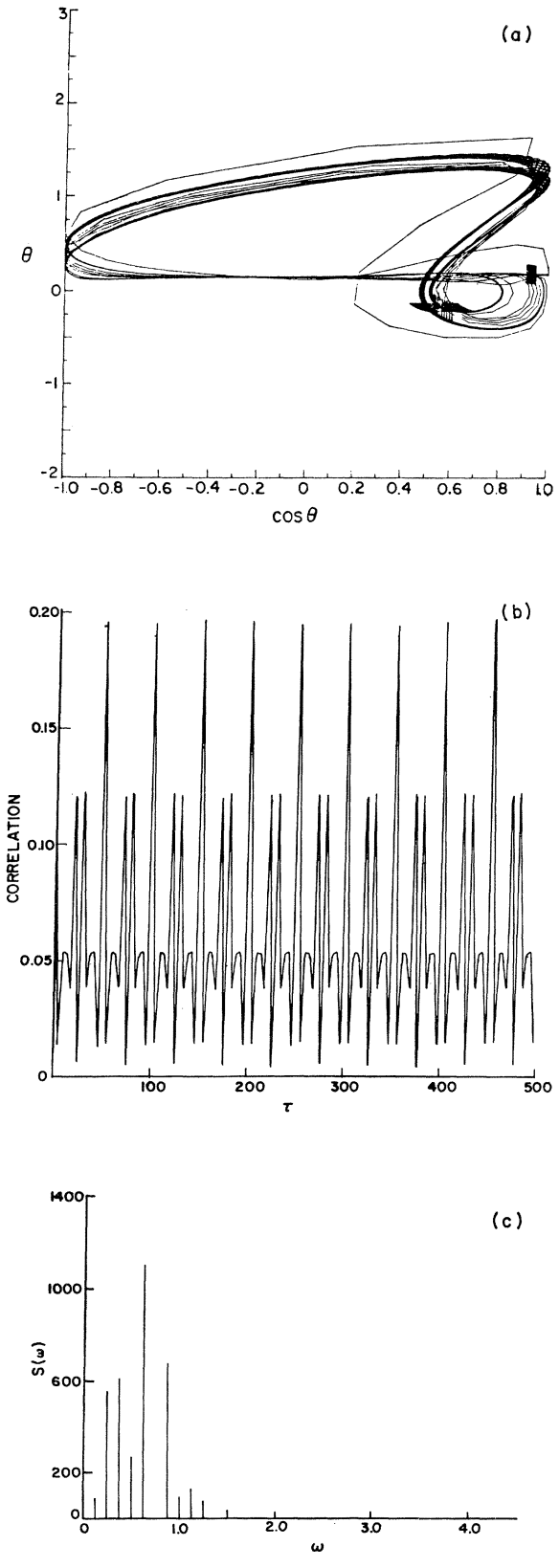

FIG. 4. (a) Phase-space plot and Poincaré section (crosses), (b) the correlation function $C(\tau)$, and (c) the power spectrum. The parameters are as in Eq. (2.6); the dc current value is $I=0.717$, a frequency-doubled running solution on step 1.

curacy and we think that it reflects some frequency-locked amplitude-modulated chaos (as discussed in Refs. 30 and 44). (See Fig. 5.)

Finally, we display in Fig. 6 an intermittent chaotic solution. Here the stochasticity is violent; as seen in Figs. 6(a) and 6(b), $C(t)$ (as well as θ) has a nonzero average (although $\langle v \rangle$ is some number less than that for the first step), with the resulting $\delta(\omega)$ part of $S(\omega)$. The continuous spectrum of $S(\omega)$ in between the peaks is prominent. $\lim_{\omega\to 0} S(\omega)=S(0)$ is finite. We call attention to the many small peaks in $S(\omega)$ in between the "δ-function" ones at $n\omega_{ex}$. These reflect a tendency towards multiple periods. In the next section we analyze the features of $C(t)$ and $S(\omega)$, which follow from the intermittent nature of this last case.

III. CALCULATIONS OF THE CORRELATION FUNCTION AND THE POWER SPECTRUM IN SIMPLIFIED STOCHASTIC MODELS FOR THE INTERMITTENT BEHAVIOR

In this section we present two models of intermittent behavior. The first one is identical to the model presented in Refs. 38 and 42 (namely, we assume random hopping between two unstable cycles). We calculate the correlation function corresponding to this model and the resulting power spectrum and comment on the meaning of the results. The second model describes a situation which is closer in nature to the "standard" picture of intermittency. We assume that the system evolves periodically for some time (which is always an integer number of periods of the forcing), then it becomes random for several periods and so on. The transitions between the "laminar" and random behavior are dictated by "known" transition probabilities as in the previous models. Finally, we analyze the meaning of the results obtained from these models. This section is divided into three subsections; the first describing the model of Ref. 1, henceforth called model A, the second presenting the other model, which we name B, and the third providing an analysis of the results.

A. Model A

This model[42] is an idealized version of the behavior of the solution of the RSJ equation, as discussed in Sec. II, when biased in the gap between two steps, e.g., step 0 and step 1. It is assumed that the solution $f(t)$ (representing $\dot{\theta}$ or the voltage across the junction) is composed of a random succession of two types of cycles, $y_0(t)$ and $y_1(t)$, each of them lasting for a time T that equals the period of the forcing. The functions $y_0(t)$ and $y_1(t)$ are assumed to be periodic with period T. They represent the periodic functions that comprise the stable solutions when the system is biased inside steps 0 and 1, respectively. When the system is biased in the gap between the steps, these two solutions are unstable and the solution hops randomly between them. The random hopping is assumed to be governed by a probability $P_{0,1}$ to hop from the y_0 cycle (after it has been completed) to the y_1 cycle and a probability $P_{1,0}$ which is defined similarly. The significance of the simplifications assumed in the framework of model A is discussed in Sec. III C.

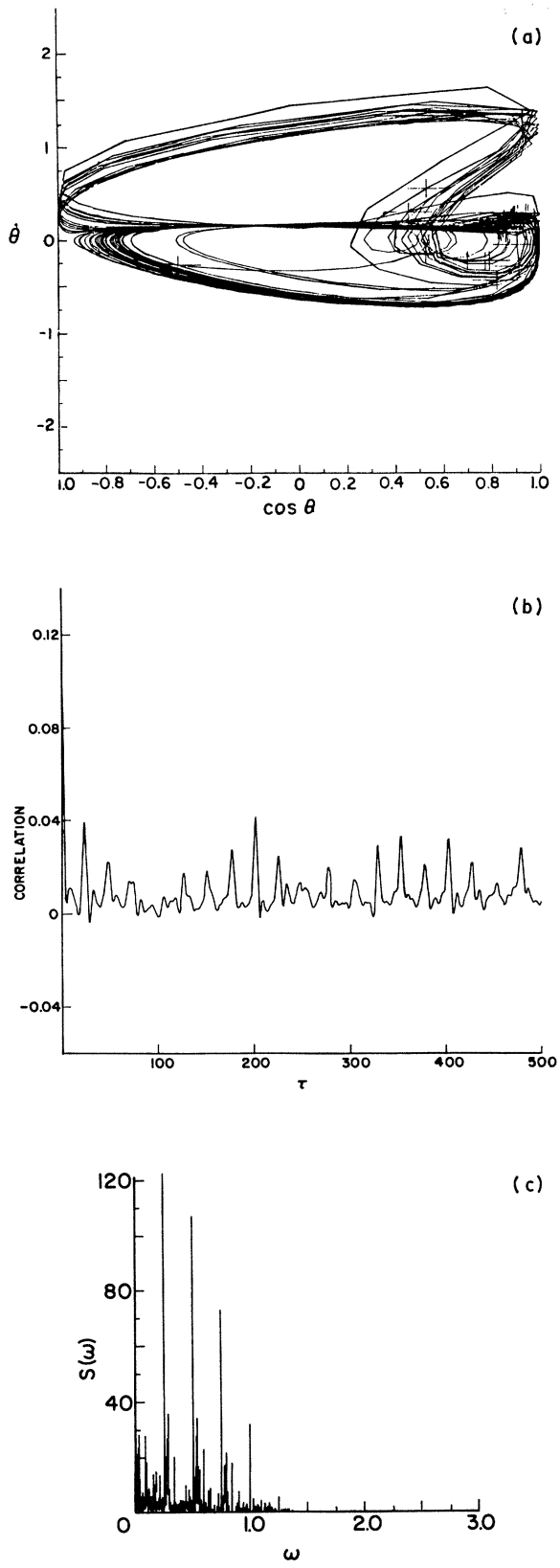

FIG. 5. (a) Phase-space plot and Poincaré section (crosses), (b) the correlation function $C(\tau)$, and (c) the power spectrum. The parameters are as in Eq. (2.6); the dc current value is $I=0.7155$, an intermittent chaotic solution.

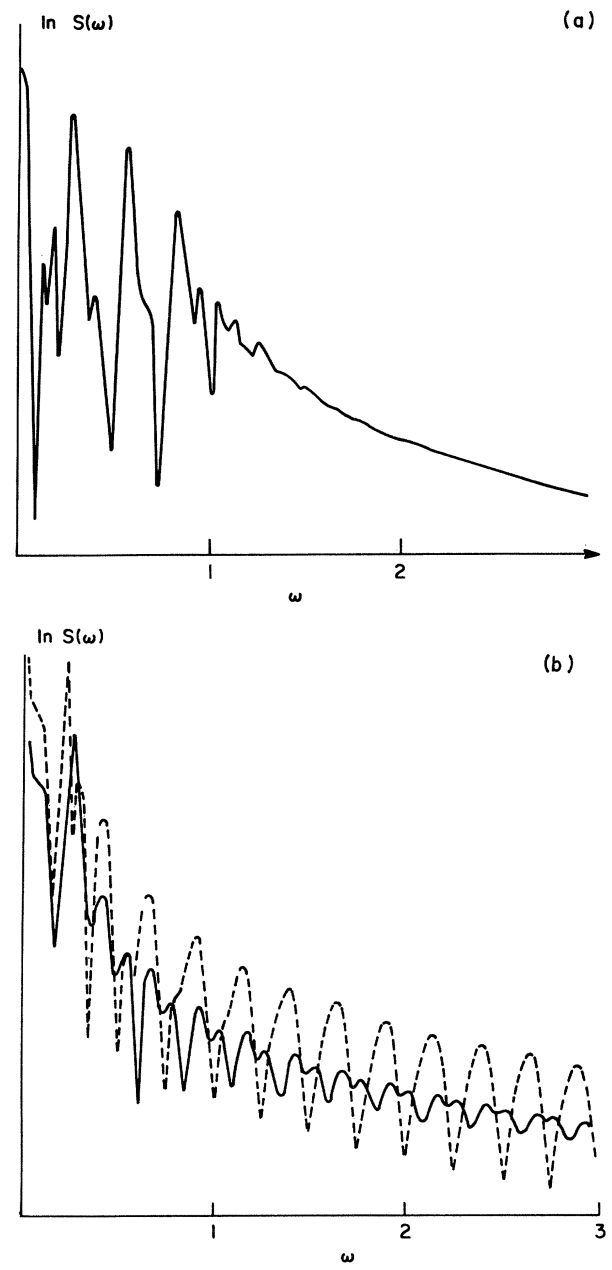

FIG. 6. Comparison of the numerically calculated $S(\omega)$ to the one obtained from Eqs. (3.15) and (3.16). The parameter values were $G=0.7$, $A=0.4$, $\omega_{ex}=0.25$; for other parameters, see text.

The correlation of the function f is defined as follows:

$$C(\tau)=\lim_{T_0\to\infty}\frac{1}{T_0}\int_0^{T_0}\langle f(t)f(t+\tau)\rangle dt\ , \tag{3.1}$$

where the average $\langle\ \rangle$ is over the previously defined probabilities $P_{0,1}$ and $P_{1,0}$. We assume, without loss of generality, that the time $t=0$ is a starting time of a cycle. Consequently, inside any time segment $(n-1)T<t<nT$, n being an integer, the solution f equals either y_0 or y_1; namely, a transition can happen only at the end of the seg-

ment. Another simplification of the calculation of $C(\tau)$ follows from the observation that the time-averaging procedure in Eq. (3.1) can be replaced by $1/T$ times an integration over the first time segment $0<t<T$. This is so because the average $\langle f(t)f(t+\tau)\rangle$ depends only on τ, $P_{0,1}$, $P_{1,0}$, and $\{t/T\}$ (identically equal to the fractional part of t/T, or the distance of t from the beginning of the segment of time in which it "resides").

In other words, $\langle f(t)f(t+\tau)\rangle$ is periodic with respect to t with period T and thus the "time average" in Eq. (3.1) can be replaced by an average over a single period. This means

$$C(\tau)=\frac{1}{T}\int_0^T\langle f(t)f(t+\tau)\rangle dt \ . \tag{3.2}$$

The variable t in Eq. (3.2) can be replaced by xT, $0\le x<1$ and the variable t can be written as $nT+yT$, where n is an integer [since obviously $C(\tau)=C(-\tau)$, it is sufficient to assume $n\ge 0$] and $0\le y<1$. Hence

$$C(\tau)=\int_0^1 dx\,\langle f(xT)f(xT+mT+yT)\rangle \ . \tag{3.3}$$

When $x+y<1$, the argument $(x+y)T+nT$ lies in the nth time segment, whereas when $1\le x+y<2$ it resides in the $(n+1)$th segment. This suggests that we divide the integration range in Eq. (3.3) into two subranges: $0\le x<1-y$ and $1-y\le x<1$. In the first of these subranges the argument of the second f is in the nth segment and in the second subrange it is in the $(n+1)$th segment. Let $P(i,j;;n)$ be the probability that $f(t)=y_i(t)$ in the first time segment *and* $f(t)=y_j(t)$ in the nth time segment ($i,j=0$ or 1). It follows from the discussion presented above that

$$C(\tau)=\sum_{i=0}^{1}\sum_{j=0}^{1}P(i,j;n)\int_0^{1-y}dx\,y_i(xT)y_j((x+y)T) +\sum_{i=0}^{1}\sum_{j=0}^{1}P(i,j;n+1)\int_{1-y}^{1}dx\,y_i(xT)y_j((x+y)T) \ . \tag{3.4}$$

Note that in writing Eq. (3.4) the periodicity of y_i has been used. The next step is the calculation of $P(i,j;n)$. This quantity can be calculated by employing the transfer-matrix method. Let us define a 2×2 matrix $\underline{F}$ by its elements: $F_{0,0}=1-P_{0,1}$, $F_{0,1}=P_{0,1}$, $F_{1,0}=P_{1,0}$, and $F_{1,1}=1-P_{1,0}$. F_{ij} is thus the probability of a transition from a cycle of type i to a cycle of type j (including the case $i=j$) after one time step. It follows that the transition probability from type-i cycle to a type-j cycle after n time segments is $(\underline{F}^n)_{i,j}$, i.e., the (i,j) element of $\underline{F}^n$. The probability $P(i,j;n)$ is the product of the probability of finding a cycle of type i, P_i, and the probability of hopping from cycle i to cycle j after n steps, $(\underline{F}^n)_{i,j}$, i.e., $P(i,j;n)=P_i(\underline{F}^n)_{i,j}$. A straightforward calculation using the right and left eigenvectors of $\underline{F}$:

$$\begin{bmatrix}1\\1\end{bmatrix}\begin{bmatrix}P_{0,1}\\-P_{1,0}\end{bmatrix}$$

and

$$(P_1,\ P_{0,1}),\ (1,\ -1)$$

with eigenvalues 1 and $Q=1-P_1-P_{0,1}$, respectively, yields

$$\begin{aligned}P(0,0;n)&=P_0^2+P_0P_1Q^n \ ,\\ P(1,0;n)&=P(0,1;n)=P_1P_0-P_1P_0Q^n \ ,\\ P(1,1;n)&=P_1^2+P_0P_1Q^n \ ,\end{aligned} \tag{3.5}$$

where (with $i,j=0,1$)

$$P_i=\frac{P_{j,i}}{P_{i,j}+P_{j,i}}=\frac{P_{j,i}}{P_{0,1}+P_{1,0}} \ . \tag{3.6}$$

Equations (3.5) can be conveniently shorthanded: $P(i,j;n)=A_{i,j}+B_{i,j}Q^n$, with obvious definitions of $A_{i,j}$ and $B_{i,j}$. Substituting this form into Eq. (3.4), we obtain

$$C(\tau)=\sum_{i=0}^{1}\sum_{j=0}^{1}A_{i,j}\int_0^1 y_i(xT)y_j((x+y)T)dx +Q^n\sum_{i,j}\left[B_{i,j}\int_0^{1-y}y_i(xT)y_j((x+y)T)dx+B_{i,j}Q\int_{1-y}^{1}y_i(xT)y_j((x+y)T)dx\right] \ . \tag{3.7}$$

As we recall, $y=\{\tau/T\}$ and $n=[\tau/T]$ (identically equal to the noninteger and integer parts of τ/T, respectively). Thus we can write

$$C(\tau)=F(\{\tau/T\})+Q^{[\tau/T]}G(\{\tau/T\}) \ , \tag{3.8}$$

where the definitions of F and G are obvious from Eq. (3.7). Thus the correlation function $C(\tau)$ is composed of a periodic part, whose period equals that of the forcing, and a decaying part. The latter part is of the form of a decaying oscillation (with period T) whose decay time is

$$\tau_0=-\frac{T}{\ln|Q|}=-\frac{T}{\ln|1-P_{0,1}-P_{1,0}|} \ . \tag{3.9}$$

Note that close to the lower side of the gap (or as the onset of the intermittent behavior is approached from within the gap) $P_{0,1}$ tends to zero and $P_{1,0}$ is close to 1. Hence τ_0 becomes very small, which means in practice that $Q^n\cong 0$ for $n\ge 1$ and the effective decay time will be one period, T. The decaying part of $C(\tau)$ is, of course, responsible for the broadband part of the power spectrum, whereas the periodic part gives rise to a set of δ functions.

An outline of the calculation of the power spectrum $S(\omega)$ corresponding to $C(\tau)$ (or its Fourier transform) has been presented in Ref. 42. Since

$$S(\omega)=\int_{-\infty}^{\infty}e^{i\omega\tau}C(\tau)d\tau=2\int_0^{\infty}\cos(\omega\tau)C(\tau)d\tau \ ,$$

we may use Eq. (3.2) and $t=xT$ as before to write

$$S(\omega)=\int_{-\infty}^{\infty}d\tau e^{i\omega\tau}\int_0^1 dx\langle f(xT)f(xT+\tau)\rangle ,$$

which can be rewritten as

$$S(\omega)=\sum_{n=-\infty}^{\infty}\int_0^1 dx\int_{(n-x)T}^{(n+1-x)T}d\tau e^{i\omega\tau}\times\langle f(xT)f(xT+\tau)\rangle . \tag{3.10}$$

Defining $\sigma=\tau-(n-x)T$, one obtains

$$S(\omega)=\sum_{n=-\infty}^{\infty}\int_0^1 dx\int_0^T d\sigma e^{i(n-x)T\omega}e^{i\omega\sigma T}\times\langle f(xT)f(nT+\sigma)\rangle . \tag{3.11}$$

Since xT is in the first time segment and $nT+\sigma$ is in the nth segment, it follows that $f(xT)$ and $f(nT+\sigma)$ can be replaced by $y_i(xT)$ and $y_j(\sigma)$, respectively, i and j being 0 or 1, averaged over the probability $P(i,j;n)$. It follows that

$$S(\omega)=\int_0^1 dx\sum_{i=0}^{1}\sum_{j=0}^{1}\sum_{n=-\infty}^{\infty}e^{i\omega nT}\int_0^T d\sigma e^{-ixT\omega}e^{i\sigma\omega}P(i,j;|n|)y_i(xT)y_j(\sigma) , \tag{3.12}$$

where $P(i,j;n)=P(i,j;-n)$ has been used.

Defining

$$f_i(\omega)=\int_0^T d\tau e^{i\omega\tau}y_i(\tau) , \quad i=0,1 \tag{3.13}$$

we obtain from (3.7)

$$S(\omega)=\frac{1}{T}\sum_{i=0}^{1}\sum_{j=0}^{1}\sum_{n=-\infty}^{\infty}P(i,j;|n|)e^{in\omega T}f_i^*(\omega)f_j(\omega) . \tag{3.14}$$

Using (3.6) the summation in Eq. (3.9) can be readily performed with the result

$$S(\omega)=\frac{2\pi}{T}|P_0f_0(\omega)+P_1f_1(\omega)|^2\sum_{n=-\infty}^{\infty}\delta(\omega T-2\pi n)+\frac{1}{T}|f_0(\omega)-f_1(\omega)|^2P_0P_1\frac{1-Q^2}{1+Q^2-2Q\cos(\omega T)} . \tag{3.15}$$

Note that the spectrum consists of a series of Bragg peaks at the driving frequency and its harmonics and a broadband spectrum. The latter vanishes when $f_0=f_1$, i.e., when the two cycles are identical, since then the "transitions" become meaningless. If either P_0 or P_1 vanishes, then the broadband part disappears as well, with an amplitude proportional to the small P_i. Of course, only one type of cycle ($j\neq i$) is present in the limit $P_i=0$. Finally, note the modulation of the broadband part by the $[1+Q^2-2Q\cos(\omega T)]^{-1}$ term.

In the zeroth step there is no phase change after the completion of a cycle (at least on the average) and in the first step the phase change per cycle is 2π. Thus for the sake of modeling the spectrum we may assume

$$y_0(t)=a_0\sin\left[\frac{2\pi t}{T}+\phi_0\right] ,$$
$$y_1(t)=a_1\sin\left[\frac{2\pi t}{T}+\phi_1\right]+\frac{2\pi t}{T} . \tag{3.16}$$

These forms are supported by a perturbative analysis.[21] Since the resulting $f_0(\omega)$ and $f_1(\omega)$ satisfy[42] $|f_0(\omega)|^2\propto 1/2\omega^2$ and $|f_1(\omega)|^2\propto 1/\omega^4$, the model spectrum decays algebraically for $\omega\gg\omega_{ex}$. In practice, of course, the spectrum will decay stronger than any power of ω as $\omega\to\infty$, where a characteristic decay frequency could be, e.g., the inverse of the (small but finite) transition time between the two cycles.[42] Another, more mathematical, way to see this would be to note[50] that $\int_{-\infty}^{\infty}\omega^{2n}S(\omega)d\omega$ should converge for all integer $n>0$, since this quantity corresponds to $\langle(f^{(n)})^2\rangle$ ($f^{(n)}$ is the nth derivative of n). The reason our model does not comply with this convergence requirement is related to the fact that $y_0(t)$ and $y_1(t)$ as well as their derivatives in Eq. (3.11) do not connect smoothly with each other. Had we "smoothed" this transition (as, of course, happens in practice) the algebraic decay would have been cut off at an ω corresponding to the width of the smoothing connection, as mentioned above.

B. Model *B*

The difference between this model and model *A* is in the fact that cycle 1 is replaced here by a random function, and, for simplicity, we assume that cycle 0 is replaced by a δ function located at the center of the period. This model has been constructed having in mind the spatial analogy of a series of finite crystallites[51] (in which the "atom" is), say, in the center between two underlying lattice points, separated by a "fluid" phase. In this case the "time" corresponds to a spatial coordinate. Alternatively, the crystallites may represent a laminar phase, whereas the fluid phase may represent intermittent bursts.

Using the terminology of Sec. III A, we define:

$$u_0^{(n)}(t)=\rho\delta(\{t/T\}-\tfrac{1}{2}) ,$$
$$u_1^{(n)}(t)=g_n(\{t/T\}) \text{ where } n=[t/T] . \tag{3.17}$$

The random functions g_n are assumed to have a constant average and a δ-function correlation:

$$\langle g_n\rangle_{av}(\{t/T\})=C ,$$
$$\langle[g_{n'}(x')-C][g_{n'}(x')-C]\rangle_{av}=k\delta(x-x')\delta_{n,n'} . \tag{3.18}$$

Equations (3.17) and (3.18) define model *B*.

As in Sec. III A, we denote by $f(t)$ the full succession of u_0's and u_1's. The corresponding power spectrum $S(\omega)$

can be written as in Sec. III A:

$$S(\omega)=\int_0^1 dx \int_{-\infty}^{\infty} dt\, e^{i\omega t}\langle f(xT)f(xT+\tau)\rangle_{\rm av} \tag{3.19}$$

and, as before:

$$S(\omega)=\sum_{n=-\infty}^{\infty}\sum_{i,j>0} P(i,j;|n|)\int_0^1 dx \int_{(n-x)T}^{(n+1-x)T} dt\, e^{i\omega t}\langle u_i^{(0)}(xT)u_j^{(n)}(xT+t)\rangle_{\rm av}$$
$$=\sum_{n=-\infty}^{\infty}\sum_{i=0}^{1}\sum_{j=0}^{1} P(i,j;n)e^{in\omega T}\int_0^1 dx\, e^{-i\omega xT}\int_0^T d\sigma\, e^{i\omega\sigma}\langle u_i^{(0)}(xT)u_j^{(n)}(\sigma)\rangle_{\rm av}\,, \tag{3.20}$$

where $\sigma=\tau-(n-x)T_0$. It follows from (3.17) and (3.18) that

$$\langle u_0^{(0)}(xT)u_0^{(n)}(\sigma)\rangle_{\rm av}=\rho^2\delta\left[\frac{\sigma}{T}-\frac{1}{2}\right] \tag{3.21a}$$

(actually no "averaging" is involved here),

$$\langle u_0^{(0)}(xT)u_1^{(n)}(\sigma)\rangle_{\rm av}=C\rho\delta(x-\tfrac{1}{2})\,,$$
$$\langle u_1^{(0)}(xT)u_0^{(n)}(\sigma)\rangle_{\rm av}=C\rho\delta\left[\frac{\sigma}{T}-\frac{1}{2}\right], \tag{3.21b}$$

and

$$\langle u_1^{(0)}(xT)u_1^{(n)}(\sigma)\rangle_{\rm av}=K\delta_{n,0}\delta\left[x-\frac{\sigma}{T}\right]+C^2\,. \tag{3.21c}$$

With the use of (3.21), the integrals in (3.20) can be performed, yielding

$$S(\omega)=\sum_{n=-\infty}^{\infty} e^{i\omega nT}P(0,0;n)\rho^2T+\sum_{n=-\infty}^{\infty} e^{i\omega nT}P(0,1;n)2c\rho T\frac{\sin(\omega T/2)}{\omega T}$$
$$+\sum_{n=-\infty}^{\infty} e^{i\omega nT}P(1,0;n)2c\rho T\frac{\sin(\omega T/2)}{\omega T}+\sum_{n=-\infty}^{\infty} e^{i\omega nT}P(1,1;n)4c^2T\frac{\sin(\omega T/2)^2}{\omega T}+P(1,1;0)2KT\,. \tag{3.22}$$

Noting that $P(1,1,0)=1$ and using Eq. (3.6) we obtain

$$S(\omega)=2\pi T\left[P_0\rho+2CP_1\frac{\sin(\omega T/2)}{\omega T}\right]^2\sum_{n=-\infty}^{\infty}\delta(\omega T-2\pi n)+P_0P_1T\left[\rho-2C\frac{\sin(\omega T/2)}{\omega T}\right]^2\frac{1-Q^2}{1+Q^2-2Q\cos(\omega T)}+2KT\,. \tag{3.23}$$

Note the three parts of the spectrum. The first is a series of Bragg peaks as before. The second part corresponds to the broadband spectrum of model *A*. The third part is a white-noise background representing the randomness of the functions g_n.

C. Analysis

The most obvious common features of the two models presented in this section are the existence of a set of Bragg peaks and a broadband part in the power spectrum. The δ functions in the power spectrum result from the existence of an "external clock"—the periodic forcing. This underlying periodicity cannot be destroyed by random or intermittent interruptions of the periodic structure, nor by the slight dephasings of the $y_0(t)$ and $y_1(t)$ functions, for example, or small changes in the periodicity around the average. In other words, a long-range order is induced in the system in the sense that $y_i(t)$ and $y_i(t+nT)$ are correlated on the average even for very large n. These questions are discussed in more detail in the next section. The broadband part or the white noise is obviously representative of the random elements of the system. In the case of two types of solutions, as in our models, the finite lifetime of each solution is responsible for the broadband part. The existence of the latter reduces in our models the weight of the δ functions part but does not endow them with a finite width.

To summarize this section, we have shown how to construct simple models for intermittent chaos (with special emphasis on periodically forced systems). We have analyzed the nature of the resulting solutions and the corresponding power spectra. Further features of the physics of the real model, which complicate the resulting correlation function and power spectrum, are discussed in the next section.

IV. CORRECTIONS TO MODEL *A* FOR INTERMITTENCY IN THE dc- AND ac-DRIVEN JUNCTION

We believe that model *A* of Sec. III is a very reasonable qualitative approximation to the correlation function of $\dot{\theta}$ and its power spectrum for the real model embodied by Eq. (2.1). The predictions of model *A* and a numerical solution of Eq. (2.1) for the power spectrum were compared in Ref. 42 for a typical intermittent chaotic case and found to be indeed in a qualitative agreement. For completeness we present here in Fig. 7 the $S(\omega)$ parts of Figs. 2 and 3 of Ref. 42, which show this comparison. Moreover, for the parameters used in Eq. (3.15) to generate the full curve in Fig. 7 (with $P_{1,0}=0.75$, $P_{0,1}=0.25$, $a_0=0.45$, $a_1=0.9$, $\phi_0=0$, $\phi_1=1.5$), we find that $\lim_{\omega\to 0}S(\omega)$ is of the order of 10^{-1}. Allowing for the sharp subharmonic peaks on top of the continuous background, the numerical result is consistent with this order of magnitude. A closer idea of the corrections needed to model *A* can be obtained, however, by looking at the numerical results for $\dot{\theta}(t)$ and $C(t)$ in Figs. 2–6 of Sec. II and comparing them to the general picture given by model *A*. The latter is seen from Eq. (3.8) for the correlation function $C(t)$ to consist of a periodic part plus another periodic part multiplied by a decay factor $Q^{[t/T]}$. It is the purpose of this section to discuss the corrections needed to bring Eq. (3.8) in better agreement with the numerically obtained $C(t)$. It will be seen that these corrections, while important and sometimes conveying some relevant physics, should not alter most of the qualitative aspects of $S(\omega)$.

Three main features displayed in the numerical results and not appearing in model *A* are as follows.

(1) A modulation of the intensity of the peaks in the long-time part of $C(t)$. An important part of this modulation is the (possibly multiple) period doubling[15,30–42,44] of the incipient periodic solutions $y_0(t)$ and $y_1(t)$. In some regions of the parameters space one may also be in the vicinity of further periods such as 3, 5, 7, etc.[52] The effects of such modulations on $S(\omega)$ are qualitatively understood.

(2) A frequency modulation exists in the solution $\dot{\theta}(t)$ in the sense that the pieces $y_0(t)$, $y_1(t)$ may be slightly displaced in time with respect to a strict periodicity, especially near the jumps between the two unstable attractors; $y_0(t)$, $y_1(t)$ are each periodic only on the average. This type of dephasing can be theoretically handled and shown, if not too large, to just reduce the periodic part of $C(t)$, i.e., to transfer some of the intensity of $S(\omega)$ from the δ functions (Bragg peaks) to the background.

(3) Correlations over times finite but larger than τ_0 of Eq. (3.9) may appear if the system has some memory and the jumps are not completely independent. It is rather straightforward to estimate the effects of such correlations.

Below, we discuss the modifications which the above effects will cause to $C(t)$ and $S(\omega)$.

A. Effects of amplitude modulation, period doubling, etc.

The simplest way to take the amplitude modulation into account is by representing it as a multiplicative correction $R(t)$ to the correlation function of model *A*, henceforth denoted as $C_0(t)$. Thus the corrected $C(t)$ will be given by

$$C(t)=R(t)C_0(t)\ , \tag{4.1}$$

where the correction function $R(t)$, should not change drastically over times much shorter than T, but it changes sufficiently between periods to account for the amplitude modulation of $C(t)$. This means that the Fourier transform of $R(t)$, $\hat{R}(\omega)$, is nonzero for $\omega \lesssim 2\pi/T \equiv \omega_{\rm ex}$. If $R(t)$ is a random function, then $R(\omega)$ will be flat as $\omega\to 0$. The $\hat{R}(\omega)$ corresponding to a period doubling will have peaks at $\omega_{\rm ex}/2$ and its multiples, with an obvious analogous behavior for higher periods. An important property of $R(t)$ is that as long as its long-time average $\langle R\rangle$ does not vanish, $\hat{R}(\omega)$ will have a δ-function part at $\omega=0$.

The corrected power spectrum $S(\omega)$ is given by a convolution of the one of the model, $S_0(\omega)$ with $\hat{R}(\omega)$,

$$S(\omega)=S_0(\omega)\otimes R(\omega)\equiv\frac{1}{2\pi}\int d\omega' S_0(\omega')R(\omega-\omega')\ . \tag{4.2}$$

Thus the Bragg peaks'-δ functions of S_0 at the integral multiples of $\omega_{\rm ex}$ will just be multiplied by $\langle R\rangle$ [which can be expected to be not far from unity if the modulation $R(t)$ is not very strong, as appears to be the case for our results]. The continuous spectrum part of $\hat{R}(\omega)$ will exist in $S(\omega)$ around all the Bragg points of S_0 with weights proportional to those of the latter. In the interesting case of a tendency for an n-multiple period, the δ-function peaks of $\hat{R}(\omega)$ at $\omega_{\rm ex}/n$ and its harmonics will now occur in a manner reminiscent of superlattice Bragg peaks, i.e., at $(m+k/n)\omega_{\rm ex}$ with k and m integers. Usually $n=2$ (period doubling) will be most important. However a very interesting case, with many subharmonics is displayed in Fig. 6. Similar phenomena, of course, occur for the periodic solutions, exhibiting period doubling, etc., as seen in Figs. 3–5.[40,41,44]

B. Effects of frequency modulation

Here we concentrate on the understanding of the effect of small random shifts in time of the functions $y_0(t)$, $y_1(t)$ on the first term [periodic part of $C(t)$] of Eq. (3.7). Such small shifts do occur in the real intermittent solutions. We shall show here that if they average to zero, the δ functions in $S(\omega)$ are not broadened but only lose intensity to the continuous background. To model this effect we take the periodic part of $C(t)$ to be the correlation of a function of the type

$$f(t)=\sum_n g(t-nT-u_n)\ , \tag{4.3}$$

where g can be taken to be nonzero only in an interval of size T and

$$\langle u_n\rangle=0\ ,\quad \langle u_n u_m\rangle=\sigma^2\delta_{nm}\ ,\quad \sigma\ll T \tag{4.4}$$

and, for simplicity, we assume a Gaussian distribution of the u's. Thus

$$\langle e^{i\omega(u_n-u_m)}\rangle = e^{-\omega^2\langle(u_n-u_m)^2\rangle/2} = \delta_{nm}+e^{-\omega^2\sigma^2}(1-\delta_{nm})\ . \tag{4.5}$$

The power spectrum of f is given by

$$S_f(\omega)=\frac{2\pi}{T}\,|g_\omega|^2\left[e^{-\omega^2\sigma^2}\sum_n \delta(\omega T-2\pi n)+(1-e^{-\omega^2\sigma^2})\right], \tag{4.6}$$

where g_ω is the Fourier transform of $g(t)$. This is similar to the familiar reduction of lattice Bragg peaks by the Debye-Waller factor ($e^{-\omega^2\sigma^2}$) and the transfer of the corresponding intensity to the continuous background. $|g_\omega|^2$ plays the role of a form factor.

C. Effects of non-Markovian correlations

If such memory effects appear, they may cause the decaying part of $C(t)$ [second, Q^n term, in Eq. (3.7)] to be modified. In particular, instead of the decay given by Eq. (3.9) a longer decay time may appear. Such an effect can indeed exist, especially near the end of the chaotic range. A hint of this effect may be noticed in Fig. 6. A long, finite relaxation time $\tau_1 \gg T_0$ will thus modify or augment the continuous part of $S(\omega)$ [last term in Eq. (3.15)] with a peak near the origin of width $\sim\tau_1^{-1}$. We, therefore, feel that the effect of the three corrections needed to model A is not large, is well defined in principle, and should not spoil the qualitative agreement with the numerical $S(\omega)$.

V. REMARKS ON THE CRITICAL BEHAVIOR

Within the model calculation of Sec. III, the critical behavior as the edge of a step i, I_i, is approached from the chaotic side is as follows. The probability to be in the ith step (which for definiteness will now be taken to be the 0 step) tends to unity. At the same time, the probability to be on the other step, $j=1$, will tend to zero. Thus defining the small dimensionless measure of the proximity to threshold

$$\epsilon=(I-I_0)/I_0\ , \tag{5.1}$$

we expect that as $\epsilon\to 0$ the probabilities P_0 and P_1 should behave like

$$P_1=A\epsilon^x,\ P_0=1-A\epsilon^x \tag{5.2}$$

where A is a numerical constant and x is a critical exponent that must be determined separately. This means that the average number of periods the solution spends around the orbits 0 and 1, n_0 and n_1, respectively, should behave, as $\epsilon\to 0$, like

$$\frac{n_0}{n_1}\sim\epsilon^{-x} \tag{5.3}$$

or since $n_1\to$const, $n_0\sim\epsilon^{-x}$, where the constancy of n_1 in the limit, which follows from our numerical data ($n_1\sim 1$–2 for $\epsilon\to 0$), means that cycle 1 is rather unstable and the instability of cycle 0 becomes marginal as $\epsilon\to 0$. In terms of the Liapounov exponent Λ_0, characterizing the latter instability, one finds $P_0=e^{-\text{const}\Lambda_0}$, and therefore Λ_0 also vanishes as

$$\Lambda_0\sim\epsilon^x \tag{5.4}$$

when $\epsilon\to 0$. For $I<I_0$, $\Lambda_0<0$ and the σ^-th steps loses its stability because $\Lambda_0\to 0-$ when $I\to I_0$ from below. Assuming the usual symmetry in the critical behavior, we expect $\Lambda_0\sim-|\epsilon|^x$ in this case.

We have roughly determined x numerically from our data, using Eq. (5.3). We find that x is on the order of 0.5–1. The value of x for the model of Ref. 37 was 0.5.

Using the results of Sec. III, we see that the parameter Q tends to a limit which is much smaller than unity as $\epsilon\to 0$. This means, as explained in Sec. III, that the effective decay time, within the model calculation, is one period. The critical behavior of $C(t)$ is thus due to, in the model of Sec. III, just the amplitude, P_0P_1 of Q^n [see Eq. (3.6) of the second, decaying, term of $C(t)$. This means that the amplitude of this contribution vanishes with P_i like ϵ^x. This leads to a similar behavior of the broadband part of $S(\omega)$ (the second term in Eq. (3.15)]:

$$S_{\text{cont}}(\omega)\sim\epsilon^x \text{ as } \epsilon\to 0\ , \tag{5.5}$$

where $S_{\text{cont}}(\omega)$ is the continuous part of $S(\omega)$.

All the above is within the approximate model of Sec. III. The possible additional broadband part of $S(\omega)$ because of the amplitude-modulated chaos on the upper edge of step 0, following the bifurcation sequence, is neglected. According to Refs. 40 and 44, that type of chaos may still have $S(0)\equiv\lim_{\omega\to 0}S(\omega)=0$. Thus Eq. (5.5) should hold for the latter limiting value.

Possible correlations in the interstep jumps, neglected in our treatment, will result in a relaxation time, similar to or in addition to τ_0 of Eq. (3.9), which may show a critical slowing down as $\epsilon\to 0$. This would entail a piece of $S(\omega)$ which will narrow into a $\delta(\omega)$ as $\epsilon\to 0$. To check this, longer simulations than ours will be needed.

VI. THE EFFECTIVE NOISE TEMPERATURE OF THE INTERMITTENT CHAOTIC STATE

Although the chaotic behavior is spontaneously generated from the deterministic dynamics of the systems, it has random jumps and a continuous power spectrum that seem to be similar to the effects of real external, e.g., thermal, noise. Thus one may say that the chaotic state has it own noise, which is equivalent in *some* respects to a thermal noise at an effective temperature T_{eff}. In fact, high effective noise temperatures have been reported for devices that might have been in chaotic states, and the connection is already suggested in Ref. 39. We emphasize that the concept of temperature in this context does not necessarily imply a full equivalence to thermal equilibrium physics or that a canonical distribution is relevant to this deterministic noise. However, some similarities to thermodynamic temperature exist and the concept seems to be useful and suggestive.

In practical terms, T_{eff} may be related to the noise gen-

erated across the resistance R.[44] Using (in a formal way) the Nyquist theorem

$$S_v(0)=\lim_{v\to 0}S_v(\omega)=4Rk_BT$$

and the Josephson voltage-frequency relation Eq. (2.2), one finds,[44] in ordinary units,

$$k_BT_{\rm eff}=\frac{1}{4}\left[\frac{\hbar}{2e}\right]^2 S_0(0)/R\ . \tag{6.1}$$

Here $S_{\dot\theta}(0)$ is the $\omega\to 0$ limit of $S_{\dot\theta}(\omega)$—the power spectrum of $\dot\theta$. In terms of our dimensionless $S(0)\equiv S_{\dot\theta}(0)/\omega_J$, we find

$$k_BT_{\rm eff}=\tfrac{1}{4}GS(0)\frac{\hbar I_j}{2e}\ . \tag{6.2}$$

(Note that $\hbar I_J/2e$ is on the order of the Josephson coupling energy of the junction, $\hbar I_J/2e\cong 2$ eV for $I_J\cong 1$ mA.) Making the estimate $S(0)\sim 10^{-1}$ for the case of Fig. 6 as discussed in Sec. IV, we find $k_BT_{\rm eff}\sim 0.02\hbar I_J/2e$. For $I_J=1$ mA this yields $T_{\rm eff}\sim 400$ K. Furthermore, when I is reduced towards I_0, $S(0)$ [Eq. (5.5)] vanishes like ϵ^x and therefore, so does $T_{\rm eff}$:

$$T_{\rm eff}\sim\epsilon^x \text{ as } \epsilon\to 0\ . \tag{6.3}$$

In Ref. 22 it was suggested that one may view the system as a two-level one, where P_0 and P_1 are given by an assumed equilibrium distribution at a temperature $T_{\rm eff}$, i.e.,

$$\frac{P_1}{P_0}=e^{-\Delta/k_BT_{\rm eff}}\ . \tag{6.4}$$

Δ was roughly estimated numerically by adding[23] to Eq. (3.1) a Langevin force $\xi(t)$ corresponding to the noise from the resistor R at an "external" noise temperature $T_{\rm ext}$, satisfying (in our dimensionless units)

$$I_Jk_B\langle\xi(t)\xi(t')\rangle=\frac{4G}{\gamma}k_BT_{\rm eff}\delta(t-t')\ , \tag{6.5}$$

where $\gamma\equiv\hbar I_J/ek_Bt$ is a dimensionless noise parameter.

Assuming the noises to be additive, one could get from the numerically determined $P_0(T_{\rm ext})$ and $P_1(T_{\rm ext})$, using an effective temperature $T_{\rm eff}+T_{\rm ext}$, an estimate of Δ. For a chaotic solution very close to that of Fig. 6, this had yielded $T_{\rm eff}$ of the order of magnitude of $\sim 10^{-3}(\hbar/2e)I_J$.[21] While this is smaller by more than an order of magnitude than the above estimate based on $S(0)$, one should remember that only two order-of-magnitude estimates have been compared here. Clearly, the assumption of additive chaotic and external thermal noises is not obviously justified. It should, however, be roughly correct since it identifies $T_{\rm eff}$ with the temperature that once it is much larger than the temperature $T_{\rm ext}$ of the thermal bath, the latter will not perturb P_0 and P_1 significantly. We also do not have any physical theory for Δ. To make sense, it should change sign around the middle of the chaotic gap, to allow for the dominant role of step 1 when I tends to the lower edge of that step. Also, for Eqs. (6.3) and (6.4) to hold simultaneously, Δ must vanish like $\epsilon^x\ln\epsilon$ as $\epsilon\to 0$, with an analogous variation near the upper edge. In any case, we find, in agreement with Kautz[44] that it is quite possible to get a $T_{\rm eff}$ due to chaos which is larger than the ambient noise temperature.

VII. CONCLUSIONS

The RSJ model (or its pendulum analog) driven by both dc and ac forces displays, in addition to its many other interesting nonlinear properties, at least two different types of chaos. A third mode of chaos has recently been suggested in Ref. 40. We have concentrated in this paper on studying the properties of the intermittent-type chaos, where the system spontaneously and stochastically jumps between two unstable orbits. The way the system approaches this kind of chaos was discussed. A model[42] for approximating the solutions, their correlation functions, and power spectra was presented and the corrections needed to make it more realistic discussed. Two definitions of the effective noise temperature for the intermittent chaotic state and some of the relations between them were briefly discussed. We believe that this type of intermittent phenomena is quite general and should occur in a variety of other physical systems.

We emphasize that a tremendous amount of work still remains to be done for an exhaustive study of this problem. The full phase diagram[39,40,41,45] giving the states of the system and the nature of the transitions among them, in the $\{G,A,\omega_{\rm ex},I\}$ parameter space is not known. Likewise, the problem can be represented by a 2D mapping,[41] via, e.g., a Poincaré section, but it is not clear how much information is lost in that process. Nor do we know the conditions under which this 2D mapping may be equivalent to a one-dimensional (1D) one—to yield the Feigenbaum universality class which is sometimes observed in our problem.[43] The interesting limiting case of the overdamped[46–49] junction, $G\to\infty$, where the model reduces to a nonautonomous first-order equation, will be the subject of further study. The Poincaré section for this problem is a 1D map and aperiodic solutions do exist both for it[47] and for the original equation.[46] The effect of, e.g., thermal noise,[53] coupled with the internally generated noise due to the chaos is important, especially near the threshold for chaos. Detailed numerical[23] studies as briefly mentioned in Sec. VI and perhaps a scaling[30,37] analysis of these effects are necessary. Finally, one would like to go on from a single junction to two coupled ones and then to various arrays, approximating the continuum 1D and 2D cases. We have already found chaos for the dc SQUID (superconducting quantum interference device), when driven by an rf source, and there can be no doubt that it exists in many different configurations.[52,54] We hope that additional experimental and theoretical work will further clarify the behavior of these intriguing systems.

ACKNOWLEDGMENTS

We are grateful to Y. Braiman, S. Fishman, P. C. Martin, P. M. Marcus, and M. Nauenberg for discussions on these problems. Two of us (I.G. and Y.I.) thank the Insti-

tute for Theoretical Physics, University of California, Santa Barbara, for the hospitality when this work was started. One of us (Y.I.) is likewise grateful to the IBM Thomas J. Watson Research Center. This research was supported by the National Council for Research and Development, Israel, and the Kernforschungsanlage, Jülich, Germany. The work of one of us (E.B.J.) was also supported by the Weizmann Postdoctoral Fellowship Institution and by the National Science Foundation Grant No. PHY-77-27084.

[1]B. D. Josephson, Phys. Lett. 1, 251 (1962); Adv. Phys. 14, 419 (1965).
[2]S. Shapiro, Phys. Rev. Lett. 11, 80 (1963); S. Shapiro, A. R. Janus, and S. Holly, Rev. Mod. Phys. 36, 223 (1964).
[3]R. Adde and G. Vernet, in *Superconductor Applications SQUID's and Machines,* Vol. 21 of *NATO Advanced Study Institute Series,* edited by B. B. Schwartz and S. Foner (Plenum, New York, 1977), Chap. 6.
[4]A. H. Dayem and J. J. Wiegand, Phys. Rev. 155, 419 (1967).
[5]D. N. Langenberg, in *Tunneling in Solids,* edited by E. Burnstein and S. Lundquist (Pergamon, New York, 1969), p. 519.
[6]P. Russer, J. Appl. Phys. 43, 2008 (1972).
[7]N. R. Werthamer and S. Shapiro, Phys. Rev. 164, 523 (1967).
[8]J. R. Waldram, A. B. Pippard, and J. Clarke, Philos. Trans. R. Soc. London Ser. A 268, 265 (1970).
[9]D. A. Weitz, W. J. Skocpol, and M. Tinkham, Appl. Phys. Lett. 31, 227 (1977).
[10]Y. Taur, P. L. Richards, and F. Auracher, in *Proceedings of the 13th International Low Temperature Physics Conference—LT13,* edited by K. D. Timmerhaus, W. J. O'Sullivan, E. F. Hammel (Plenum, New York, 1974), Vol. 3.
[11]C. A. Hamilton and E. G. Johnson, Jr., Phys. Lett. 41A, 393 (1972).
[12]V. N. Belykh, N. F. Pedersen, and O. H. Soerensen, Phys. Rev. B 16, 4853; 16, 4860 (1977).
[13]R. K. Kirschman, J. Low Temp. Phys. 11, 235 (1973).
[14]N. F. Pedersen, M. R. Samuelson, and K. Saermark, J. Appl. Phys. 44, 5120 (1973).
[15]N. F. Pedersen, O. H. Soerensen, B. Dueholm, and J. Mygind, J. Low Temp. Phys. 38, 1 (1980).
[16]H. Lübbig and H. Luther, Rev. Phys. Appl. 2, 20 (1979).
[17]R. A. Kamper, in *Superconducting Applications SQUID's and Machines,* Ref. 3, p. 189.
[18]M. T. Levinsen, R. P. Chiao, M. J. Feldman, and B. A. Tucker, Appl. Phys. Lett. 31, 776 (1976).
[19]R. L. Peterson and D. G. MacDonald, IEEE Trans. Magn. MAG-13, 887 (1977).
[20]R. L. Kautz, J. Appl. Phys. 52, 3528 (1981).
[21]Y. Braiman, E. Ben-Jacob, and Y. Imry, in *SQUID 80,* edited by H. D. Hahlbohm and H. Lübbig (Walter de Gruyter, Berlin, 1980).
[22]E. Ben-Jacob, Y. Braiman, R. Shainsky, and Y. Imry, Appl. Phys. Lett. 38, 10 (1981).
[23]Y. Braiman, E. Ben-Jacob, and Y. Imry, IEEE Trans. Magn. MAG-17, 784 (1981).
[24]J. Kadlec and K. H. Gundlach, *Superconductor Applications SQUID's and Machines,* Ref. 3.
[25]D. E. McCumber, J. Appl. Phys. 39, 3113 (1968).
[26]W. C. Stewart, Appl. Phys. Lett. 12, 277 (1968).
[27]G. Gruner, A. Zawadowski, and P. M. Chaikin, Phys. Rev. Lett. 46, 511 (1981).
[28]R. W. Henry and D. E. Prober, Rev. Sci. Instrum. 52, 912 (1981).
[29]J. A. Yorke and E. D. Yorke, J. Stat. Phys. 21, 263 (1979).
[30]M. J. Feigenbaum, J. Stat. Phys. 19, 25 (1978); 21, 669 (1979).
[31]R. Shaw, Z. Naturforsch. 36a, 80 (1980).
[32]B. A. Huberman and J. P. Krutchfield, Phys. Rev. Lett. 43, 1743 (1979).
[33]P. Collet and J.-P. Eckmann, *Iterated Maps on the Interval as Dynamical Systems* (Birkhauser, Boston, 1980).
[34]G. Ahlers and R. W. Walden, Phys. Rev. Lett. 44, 445 (1980).
[35]P. Manneville and Y. Pomeáu, Phys. Lett. 75A, 1 (1979).
[36]E. N. Lorenz, J. Atmos. Sci. 20, 130 (1963).
[37]J. Hirsch, B. A. Huberman, and D. J. Scalapino, Phys. Rev. A 25, 519 (1982).
[38]Y. Aizawa, Prog. Theor. Phys. 68, 64 (1982).
[39]B. A. Huberman, J. P. Krutchfield, and N. Packard, Appl. Phys. Lett. 37, 750 (1980).
[40]D. d'Humieres, M. R. Beasley, B. A. Huberman, and A. Libchabe (unpublished).
[41]A. H. MacDonald and M. Plischke, Phys. Rev. B 27, 201 (1983).
[42]E. Ben-Jacob, I. Goldhirsch, Y. Imry, and S. Fishman, Phys. Rev. Lett. 49, 1599 (1982).
[43]See, e.g., J.-C. Roux, J. S. Turner, W. D. McCormick and H. L. Swinney, in *Nonlinear Problems: Present and Future,* edited by A. R. Bishop (North-Holland, Amsterdam, 1981).
[44]R. L. Kautz, J. Appl. Phys. 52, 6241 (1981).
[45]N. F. Pedersen and A. Davidson, Appl. Phys. Lett. 39, 830 (1981).
[46]I. Goldhirsch, Ann. N.Y. Acad. Sci. 404, 48 (1983).
[47]J. R. Waldram and P. H. Wu, J. Low. Temp. Phys. 47, 363 (1982).
[48]M. J. Renne and D. Polder, Rev. Phys. Appl. 9, 25 (1974).
[49]I. Goldhirsch (unpublished).
[50]We are indebted to Professor P. C. Martin for discussions and to Dr. D. Farmer for correspondence on this point.
[51]See, for example, *Ordering in Two Dimensions,* edited by S. K. Sinha (North-Holland, New York, 1980).
[52]E. Ben-Jacob, Y. Imry, and P. M. Marcus, unpublished results for the voltage driven junction [see Solid State Commun. 41, 161 (1982)].
[53]E. Ben-Jacob, D. J. Bergman, and Z. Schuss, Phys. Rev. B 25, 519 (1982), and unpublished.
[54]K. Fesser, A. R. Bishop, and P. Kumar (unpublished).